J. Exp. Biol. (1974), **60**, 207–221
With 1 plate and 5 text-figures
Printed in Great Britain

ATTACHMENT OF *GIARDIA* – A HYDRODYNAMIC MODEL BASED ON FLAGELLAR ACTIVITY

BY D. V. HOLBERTON
Department of Zoology, University of Hull, Hull

(*Received 22 March* 1973)

INTRODUCTION

Alternative mechanisms have been proposed to account for the attachment of the gut flagellate *Giardia* to the intestinal wall of its host. The morphology of this protozoan is dominated by a large ventral disc which in traditional description functions as a sucker. However, recent electron-microscope studies of *G. muris* have conflicted in their interpretation of the role of this disc and structures associated with it.

Friend (1966) considered the disc to be a supporting pontoon without suction properties and suggested that a ventro-lateral flange around the disc effects attachment through a mechanical grasping action. The evidence for this view is found in the close approach of the ventro-lateral flange and host-cell surfaces and in the presence within the flange of a flexible plate showing ultrastructural similarity to paramyosin-containing filaments precipitated from invertebrate muscle proteins.

Reasons for questioning this hypothesis have been given in an earlier paper which also sought to reaffirm suction pressure within the disc as the force promoting attachment (Holberton, 1973). The origin of this force is a fluid flow maintained beneath the cell by continuous beating of a ventral pair of flagella. The suction pressure developed hydrodynamically is transmitted hydrostatically through a portal in the disc rim to the suction disc cavity.

The *Giardia* attachment mechanism is clearly an unusual one; but, set alongside the ultrastructural studies, to correctly identify these forces raises questions of wider implication. For instance, the suction disc is supported by a cytoskeleton of unusually cross-bridged microtubules. The same microtubules are linked by side-arms to the ventral plasma membrane. To what extent may this molecular architecture be related to local deforming forces of appreciable magnitude?

Originally it was shown by empirical argument that a negative pressure gradient will be set up by changes in the velocity and viscous stress parameters of the flow (Holberton, 1973). The approach used was a qualitative one, a simply analogy to the Bernouilli analysis of ideal fluid flow based on the principle of energy conservation along a streamline. In the present paper this analogy is discarded in favour of a more rigorous model derived from the fundamental equations of viscous flow to demonstrate the origin of suction pressure beneath the cell. The analysis predicts the separate contributions of velocity gradient and viscous stress gradient components to the net suction pressure, and allows an appraisal of the extent to which maintained adhesion is independent of fluctuations in flagellar beat rate or changing wave parameters.

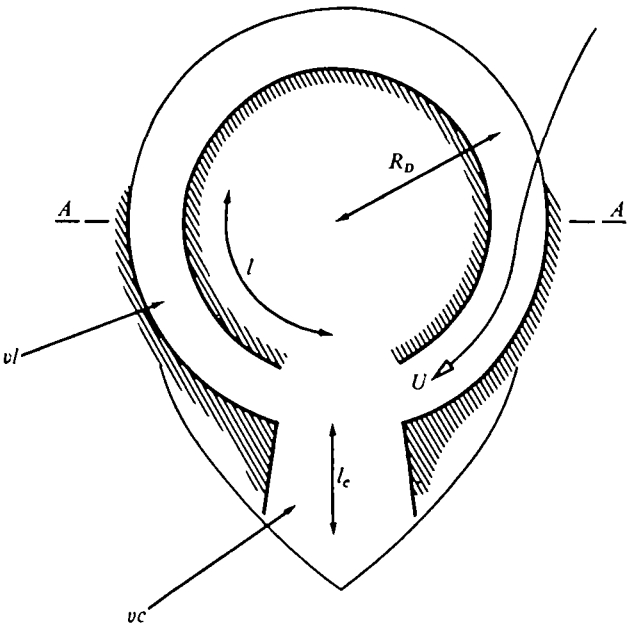

Text-fig. 1. The ventral aspect of *Giardia* attached to glass. Contact of cell and substrate (indicated by hatching) at the disc rim and ventro-lateral flange margin defines a Y-shaped channel of ventro-lateral (*vl*) and ventro-caudal (*vc*) sections, respective lengths l and l_c μm. The open-headed arrow indicates a single streamline of achieved fluid velocity u cm sec^{-1}.

MATERIALS AND METHODS

The calculations of this paper are based on measurements from electron micrographs of *Giardia muris* fixed *in situ* on the wall of the small intestine of the mouse, and from phase-contrast micrographs of freshly excised trophozoites attaching to glass slides. Electronic flash exposures were used to 'freeze' flagellar movement, a rotating aperture stroboscope to determine beat rate. These methods have been described in greater detail elsewhere (Holberton, 1973).

OBSERVATIONS

Although *Giardia* is an organism that has received little experimental attention, its detailed morphology has recently been described (Holberton, 1973). Briefly, in plan optical section the trophozoite appears kite-shaped, the broad anterior of the cell derives from the large circular and concave adhesive disc of the ventral surface. The translational movement of the detached cell is saltatory and erratic, the outcome of the combined motion of eight beating flagella. The cell body tends to rotate slowly about the longitudinal axis during this irregular progression. Once attached to glass the flagella, with the exception of the two ventral flagella, beat intermittently, and it is the continuous undulations of this pair that result in a flow of fluid around the attached cell.

The ventral axonemes arise as free flagella within the sucking disc, pass through the portal in the posterior rim of the disc, and are housed in a shallow longitudinal groove

Table 1. *Wave parameters of ventral flagella at various frequencies from individual protozoans attached to glass*

Frequency (Hz)	Mean wavelength, λ (μm)	Mean amplitude, η (μm)	ηk	Wavelength non-uniformity $(\lambda/2)_{max}/(\lambda/2)_{min}$
18	5·1	0·71	0·87	1·7
12	4·7	0·74	0·99	1·7
9	4·5	0·98	1·37	1·8
7	4·2	1·03	1·54	2·2
2·5	3·9	1·28	2·03	2·2

of the ventro-caudal surface (Pl. 1, fig. 1). This groove is continued forward to either side of the sucking disc by the arched profile adopted by the ventro-lateral flange, a flexible cytoplasmic lip flanking the disc perimeter. The flange is raised at the front of the cell but meets the substrate laterally, so that with general contact between the ventral surface and the substrate (glass or gut epithelium) the sucking disc cavity is sealed at its rim leaving a Y-shaped channel beneath the cell (Text-fig. 1). The arms of the Y (ventro-lateral flanges) meet at a point immediately behind the disc portal (the channel throat), while the stem of the Y (ventro-caudal channel) encloses the beating flagella. In the attached cell, fluid movement is led entirely through this channel, but when an unattached cell initially approaches a substrate, part of the flow passes through the open aperture of the unsealed ventral disc and may contribute directly to the attachment event. Such an effect is ignored by the following analysis which rests on the premise that, since detachment follows the interruption of flagellar activity, maintained attachment may be separately examined, solely as a steady-state function of the constant fluid flow through the ventral channel.

On a deformable substrate, contact between host and protozoan cell surfaces ultimately becomes intimate (to within 20 nm at the disc rim) and it is possible that short-range forces, such as might normally operate between cells of a tissue (Curtis, 1967), may prevail. Since the host-surface cell is distorted during attachment, the effectiveness of forces of close adhesion will depend on the size of restoring forces within the deformed cell cortex; for instance, the extent to which initial strains are truly elastic or might be diminished by the viscous flow of cortical cytoplasm. However, totally effective close adhesion would deny reversibility to the attachment mechanism, and the finding of a conserved sinusoidal waveform of the ventral flagella in electron micrographs suggests a requirement for continuous flagellar beating *in situ* on the gut wall as well as on glass substrates.

Observation and photography of the base-to-tip wave propagated by the double shaft are aided by the sessile habit of the organism, and all data relating to flagellar activity used in this analysis are taken from organisms attached to glass. Some examples of wave parameters determined at different frequencies are given in Table 1. It should be emphasized that these results are from organisms photographed in crude scrapes from the intestinal mucosa without control of medium viscosity or temperature. In particular, since the temperature of the microscope stage was some 10–15 °C below body temperature, the frequencies recorded are likely to average lower than in the gut. As these simple slide preparations age, the flagellar beat of individual protozoans slows; none the less many organisms remain attached until the frequency falls below 2 Hz.

Table 1 demonstrates a range of flagellar activity compatible with attachment without implying a relationship between frequency and any other parameter beyond a trend toward shorter wavelength and greater amplitude at lower frequencies. Except at low frequencies synchrony of the motions of the two ventral flagella is complete. The circularity of the waveform changes from near-helical in the detached organism to near-plane as the cell and substrate are drawn closer together and as the beat slows. The use of the simple numerical data in the equations that follow is further qualified by the observation that the two-dimensional projection of the waveform is more nearly an arc-line or meander than a true sine wave (Silvester & Holwill, 1972) and is non-uniform (in most cases both the wavelength and the wave amplitude increase toward the tip). Accordingly, the parameters of Table 1 are expressed as 'means' (mean wavelength of a non-uniform wave is the length of the waveform divided by the number of waves; mean amplitude the numerical average of individual peak amplitudes). A measure of wavelength non-uniformity is given by the ratio of the largest and smallest half-waves of one waveform.

THEORETICAL REALIZATION OF THE ATTACHMENT MODEL

Suction pressure

The model assumes that one effect of flagella beating within the ventral channel is to generate a suction pressure behind the ventral disc. The two propositions of the model are:

(i) That flow through the ventral channel leads hydrodynamically to a progressive fall in fluid pressure.

(ii) That at a point in the flow immediately behind the disc the achieved magnitude of the suction pressure is such that, applied to the disc face, it will deform the surface of the underlying cell to the observed degree.

Clearly, since the pressure far ahead of the channel flow may be assumed uniform (the static pressure around the cell) and must have a single value at the point of confluence of the two lateral channels, these two channels are hydrodynamically equivalent and the same drop in pressure is experienced in each. The problem reduces to a solution for changes in the flow parameters beneath the ventro-lateral flange on one side of the disc. The very small dimensions of this channel and the low velocity of the flow argue a situation of viscous flow with negligible inertial forces (a Reynolds number of the order 10^{-4}). Previous authors have drawn on the predominance of viscous forces in the motion of microstructures to derive equations describing the propulsion of flagellated cells (Taylor, 1951; Holwill, 1966). In the present instance the low Reynolds number means that the flow through the ventral channel is essentially laminar, and that a satisfactory solution of the general dynamical equations for real fluids (Navier–Stokes equations) may be found in a rearrangement of the familiar Hagen–Poiseuille equation relating the viscous resistance to flow in a tube to the pressure difference between its ends. For a tube section of length l, and radius r, the pressure difference sustained by a flow of maximum (axial) velocity, u_{max}, is

$$\Delta P = \frac{4u_{max}\mu l}{r^2}, \tag{1}$$

where μ is, as usual, the absolute viscosity.

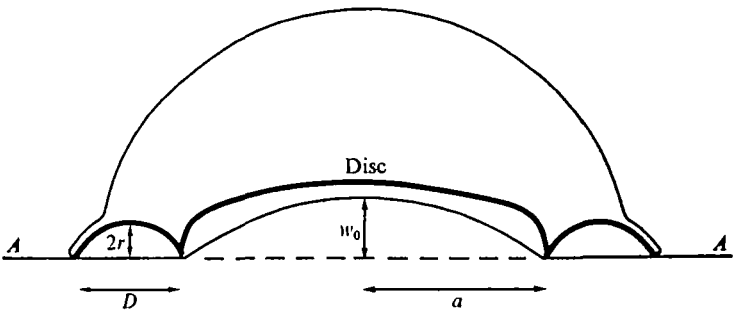

Text-fig. 2. *Giardia* attached to a deformable substrate in diametrical cross-section (*A–A* of Text-fig. 1). Ventro-lateral channel shown approximately semicircular with dimensions D and $nD = 2r$; a, radius of suction disc; w_0, substrate deformation at the disc centre.

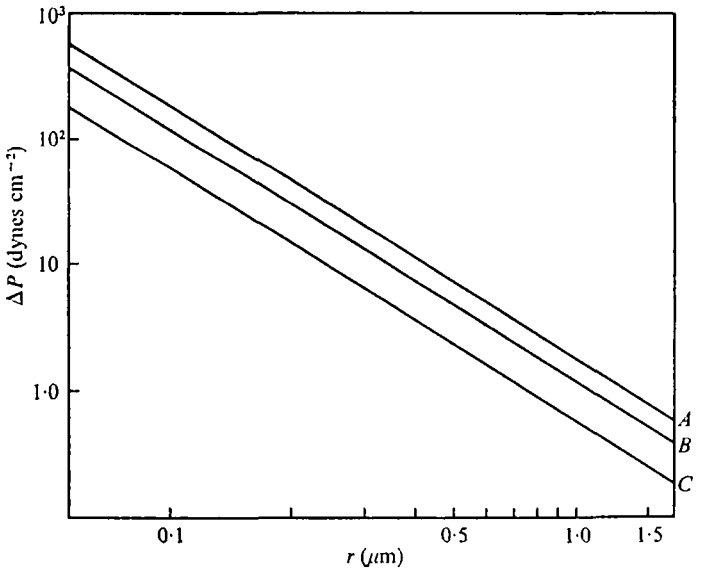

Text-fig. 3. Dependence of suction pressure (ΔP) on the ventro-lateral channel dimension r, for various channel lengths (l). *A*, $l = 0{\cdot}7\pi R_D$; *B*, $l = 0{\cdot}3\pi R_D$. *C*, $l = 0{\cdot}1\pi R_D$. From equations (2) and (11), assuming helical flagellar waves of parameters; frequency, 20 Hz; wavelength (λ), 5 μm; amplitude (η), 0·75 μm; d/λ, 0·06; m, 5. R_D is taken as 4 μm; l_0 as 2·5 μm (see Pl. 1, fig. 1).

But this is the expression for a tube of uniform circular cross-section whereas the cross-section of the *Giardia* lateral channel is irregular (Pl. 1, fig. 2). From electron-micrographs the channel profile is more nearly semi-circular or elliptical; in particular the horizontal dimension, D (Text-fig. 2), can exceed the vertical separation between flange surface and substrate, $2r$, by a factor of 3. It is the smaller dimension that most profoundly determines the viscous resistance developed, and is the more significant parameter affecting the magnitude of the suction pressure. In the extreme, discounting the effect of the sides of the channel, the situation compares to Poiseuille flow between two flat plates with a solution similar in form to equation (1), but with the numerical constant reduced in value from 4 to 2 (Duncan, Thom & Young, 1970). The flow

through the lateral channel is bracketed by these two cases and may be most closely modelled by assuming an elliptic cross-section having a ratio n of minor axis to major axis, and using the general solution:

$$\Delta P \simeq \frac{2(1+n^2)\, u_{max}\, \mu l}{r^2}. \tag{2}$$

As a function of the achieved suction pressure, attachment of *Giardia* will be most sensitive to the distance separating the ventro-lateral flange from the substrate surface, since this appears as a very small dimension taken to the second power (Text-fig. 3).

In an earlier paper it was shown that the accumulating viscous resistance and the positive velocity gradient both favour the development of a suction pressure. In fact although the flow accelerates from zero velocity at infinity to a maximum value in the *Giardia* channel, the component of the suction pressure arising from this source is relatively small. It is given by Pai (1956) as about $2{\cdot}2(\rho/2)(Q/\pi r^2)$ for a well-rounded tube entrance, where Q is the volumetric flow rate and ρ is the fluid density. Assigning Δp to this correction, and if ΔP is the suction pressure calculated from the viscous flow equation,

then
$$Q = \frac{\pi r^4}{8\mu l}\Delta P, \tag{3}$$

and
$$\frac{\Delta p}{\Delta P} = \frac{2{\cdot}2\rho r^2}{16\mu l}. \tag{4}$$

In *Giardia* r is less than 1 μm, leading to the conclusion that the velocity change effect accounts for, at most, 0·02 % of the final suction pressure.

Activity of the ventral flagella

For an organism in a medium of constant viscosity, the magnitude of the suction pressure follows (equation 2) from a shape factor of the ventral channel, the ratio $(1+n^2)/r^2$, and the mean axial velocity, u_{max}, of the flow. The pressure will also vary with the length of the channel, but in practice the simple relationship implied by equation (2) alone is misleading since the achieved flow velocity is governed by the resistance of motion, or drag, offered by the walls of the inert channel system, and it will be shown below that the drag itself is a function of the channel length.

The flow velocity of a fluid movement around a sessile flagellated cell may be compared to the translational velocity of a similar micro-organism propelled by flagella.

A number of authors have examined the forces on a flagellum in a free fluid and their equations allow an estimate of fluid velocity from flagellar wave parameters. But this strategy cannot be rigorously extended to *Giardia* where fluid motion is constrained within a tube of size comparable to flagellar wavelength, and for which a complete solution is unattainable. Nevertheless, in the absence of an experimental measurement, flow velocity is calculated below from uncorrected equations recognizing that the result is acceptable only to an order of magnitude. As the width of the ventro-caudal channel approaches twice that of either lateral channel, it will be assumed that no additional contraction of the flow is imposed at the junction, and that the law of continuity is satisfied by the same mean velocity in each branch of the channel system. A relationship between the translational velocity of a flagellated micro-organism and the

velocity of propagation of flagellar waves has been derived by Gray & Hancock (1955) for plane sinusoidal waves, and by Holwill & Burge (1963) for a helical sine wave. Since, if the translation velocity is assumed uniform, no net force is resolved along the axis of motion, the drag of an inert cell body moving at this velocity may be equated with the component along this axis of the total viscous resistance offered by the medium to the flagellar wave motion. By this means account has been taken of the extra resistance to motion contributed by an inert spherical body leading to the following expressions for translational velocity,

$$\frac{u_{\max}}{V_w} = \frac{\frac{1}{2}\eta^2k^2}{1+\eta^2k^2-(1+1/2\eta^2k^2)^{\frac{1}{2}}\,[ln(d/2\lambda)+1/2]\,(3R_B/m\lambda)}, \tag{5}$$

for plane sine waves (Gray & Hancock, 1955, rearranged from equation (xxv)), and

$$\frac{u_{\max}}{V_w} = \frac{\eta^2k^2}{1+2\eta^2k^2-(1+\eta^2k^2)^{\frac{1}{2}}\,[ln(d/2\lambda)+1/2]\,(3R_B/m\lambda)} \tag{6}$$

in the case of helical waves (Holwill & Burge, 1963, equation (13)). In these equations V_w is the flagellar wave velocity, λ and η are respectively the average wavelength and amplitude of the wave, $k = 2\pi/\lambda$, R_B is the radius of the inert body, d the width of the flagellar filament, and m is the number of wavelengths resolved in the direction of propulsion.

The same approach can be extended to the *Giardia* channel flow replacing the expression for the viscous retarding force of a spherical body by an alternative term appropriate to the geometry of the channel system. For laminar flow in a circular pipe of diameter $2r$ and length L, the drag of the inert wall is

$$D = \tau_m w L, \tag{7}$$

where w is the pipe perimeter and τ_m the mean frictional stress on the pipe wall in the axial direction is proportional to the non-dimensional drag coefficient, and is given by Duncan *et al.* (1970) (equation 7.68):

$$\tau_m = 4\mu\bar{u}/r. \tag{8}$$

The mean velocity $\bar{u}$ is half the axial velocity $u_{\max}$ (parabolic velocity profile); the total drag may then be written

$$D = 4\pi\mu L u_{\max}. \tag{9}$$

(This last expression compares to $D = 6\pi\mu a u$, the Stokes expression for the drag of a moving sphere of radius a.) For the general case of a tube of elliptic section, by the same argument as justifies equation (2), it is more correct to write,

$$D = 2[(1+n^2)/n]\text{-}\pi\mu L u_{\max}.$$

Thus for a flagellum beating within a tube of length L the appropriate equations of fluid motion derived from equations (5) and (6) are respectively

$$\frac{u_{\max}}{V_w} = \frac{\frac{1}{2}\eta^2k^2}{1+\eta^2k^2-(1+1/2\eta^2k^2)^{\frac{1}{2}}\,[ln(d/2\lambda)+1/2]\,[(1+n^2)L/nm\lambda]} \tag{10}$$

and

$$\frac{u_{\max}}{V_w} = \frac{\eta^2k^2}{1+2\eta^2k^2-(1+\eta^2k^2)^{\frac{1}{2}}[ln(d/2\lambda)+1/2]\,[(1+n^2)L/nm\lambda]}. \tag{11}$$

Here L is a convenient parameter representing the total inert surface contributing the

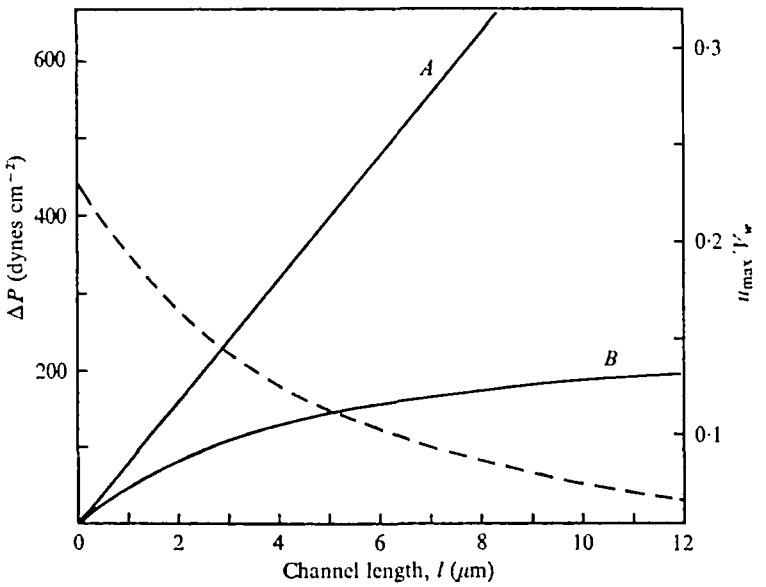

Text-fig. 4. Showing the decline in fluid velocity expressed as the ratio u_{max}/V_w (dashed curve) with increasing channel drag (as a function of channel length) and its effect on the achieved suction pressure (*B*). Curve *A* plots the linear dependence of suction pressure on channel length (*l*) expected from equation (2) for the hypothetical case of constant fluid velocity. Flagellar wave parameters and channel parameters as for Text-fig. 3.

retarding force. Whereas in *Giardia* the effective suction pressure is generated within the length of either lateral channel, this 'skin friction' is offered by the entire ventral channel system. The dimension relevant to the drag equation will be some function of component channel lengths and will depend on relative cross-section (the value of n in each channel). The simplest case is for channels of similar ellipticity when $L = 2l + lc$, if lc is the length of the hydrodynamically effective section of the ventro-caudal channel. Taking representative values for the parameters of equation (11), we find that though the greater drag force retards fluid velocity, a longer lateral channel will enhance the final suction pressure. Over a sixfold range of values for l, approaching the limit when l is half the disc perimeter ($l = \pi R_D/6 \rightarrow \pi R_D$), increasing channel drag reduces the flow velocity by approximately half, none the less there is a threefold gain in suction pressure (Text-fig. 4).

Effect of suction pressure on the gut epithelium

As can be seen from electron micrographs (Pl. 1, fig. 2), the effect of a negative pressure beneath the ventral disc of an attached *Giardia* is to draw into a surface of curvature the underlying gut cell surface, in much the same way as the cortices of various free cells have been experimentally deformed in the cell elastimeter. *Giardia* will act as a natural micro-elastimeter to the gut epithelium if this effect can be quantified. Conversely, a complete mathematical solution for the cell elastimeter that relates suction pressure to the induced deformation will allow an independent estimate of the suction pressure produced by *Giardia* if the elastic properties of the substrate are known or can be reasonably assumed.

The elastimeter technique was originally used by Mitchison & Swann (1954) to measure the rigidity or 'stiffness' of the cortical plasm of unfertilized and cleaving sea-urchin eggs. From the linear pressure/deformation curve, these authors inferred the presence of a relatively thick (compared to the plasma membrane) cortex apparently obeying Hooke's law. Though this structure could be reasonably modelled by thin-walled rubber spheres (leading by similarity analysis to a value of Young's modulus for the egg cortex) a rigorous theory of the elastimeter was found to be intractable when a treatment of the complete cortex was attempted within the general theory of spherical shells. But the principal stresses were identified as bending stresses (at the lip of the elastimeter and arising from the decreasing radius of curvature of the enclosed portion of the surface), rather than tangential membrane stresses in the cortex as a whole. In these circumstances the local stresses can be satisfactorily modelled by regarding the region of the cortex beneath the elastimeter tip as an independent plate and examining the stresses resulting from a change of curvature under load. A similar approach would seem to have been adopted by Selman & Waddington (1955) in calculating Young's modulus for the newt egg cortex from a formula for the clamped end-plate of a pressurized cylinder.

Turning to the gut cell, as part of a continuous epithelium each cell is effectively anchored laterally to its neighbours, so that any deformation of the free surface by *Giardia* is more evidently a local effect. The formal model is that of a thin circular plate, clamped at its edges, and loaded normally and uniformly over its surface. In this instance the load is taken to be the suction pressure of the *Giardia* disc; a positive internal pressure of the gut cell acts in the same direction, but (if present) is without measurable effect on the undisturbed cell cortex and can be ignored. The nature of the significant stresses in such a plate depend very much on its thickness in relation to other dimensions, in particular the ratio of the central deflexion at equilibrium (w_0) to the thickness of the plate (h) (Text-fig. 3; Pl. 1, fig. 2). For small deflexions it may be assumed that the middle plane of the plate suffers deformation to a negligible degree and the load may be approximately equated with the bending stresses of a relatively rigid plate in the linear theory of 'pure bending'. Should the edges of the plate be immovable in its plane (clamped) then additional tensile stresses (membrane stresses) arise in counteraction to the load. For instances of small deflexion, membrane forces may be practically disregarded, but for the large deflexions account must be taken of strain in the mid-plane leading to non-linear equations and a more complicated solution. In these cases a given load is opposed at equilibrium partly by flexural rigidity and partly by membrane action. In the extreme example of a very thin plate resistance to bending may be discounted and the tangential stresses of membrane behaviour alone may be regarded as carrying the load.

Whether or not the elementary (small deflexion) theory should be applied to a specific problem can be judged from the percentage error introduced by neglecting the non-linear terms of the more general equation. An approximate formula for large deflexions given by Timoshenko & Woinowsky-Krieger (1959) may be written

$$\frac{qa^4}{Eh^4} = \frac{1}{B}\,\frac{w_0}{h}\left[1 + A\frac{w_0^2}{h^2}\right], \tag{12}$$

where q is the applied force, a the radius of the plate, E is Young's modulus and A and

B are numerical constants appropriate to the boundary conditions and material of the plate. $A(w_0^2/h^2)$ is then the non-linear correction to allow for stretching of the mid-plane. It is clear that as the ratio w_0/h decreases the correction becomes progressively smaller. For instance, with A assigned values approaching unity, the correction is less than 4% when the ratio is 1/5. On the other hand, when the central deflexion is of the same order as plate thickness, use of the uncorrected linear theory would underestimate by 50% the load appropriate to that deflexion. Micrographs of the deformed gut cell suggest that the central deflexion may be greater than the thickness of the effective cortex (w_0/h lies between 1 and 1·4) and clearly the elementary theory cannot be satisfactorily applied to deflexions of this order.

The numerical constant A takes a value that depends on the edge condition of the plate, whether clamped, fixed, or free to move, and on Poisson's ratio for the material of the plate. This value is determined rigorously only by extended calculation and ultimately as the approximation of an infinite series (Prescott, 1924). A shorter route is provided by the 'strain energy method' (Timoshenko, 1937), in which the final shape assumed by the deflected plate is assigned a reasonable equation and this defines an equilibrium between the work of the applied load and the potential energy of the plate (the combined strain energies of bending and of stretching the mid-plane). Assigning suitable edge conditions gives alternative solutions of the relevant energy equations and in this way the final expression for the central deflexion (w_0) may be appropriately modified. For a rigidly clamped plate in which the boundary conditions of zero radial displacement at the centre and the edge of the plate are satisfied, Timoshenko (1937) offers a solution computed for the value of Poisson's ratio, $\nu = 0{\cdot}3$. Re-working these equations (pages 431 *et seq.* in that reference) for $\nu = 0{\cdot}5$, a value considered reasonable for biological tissues (Mitchison & Swann, 1954; Yoneda, 1964; Mela, 1967) we derive.

$$\frac{qa^4}{Eh^4} = \frac{16}{3(1-\nu^2)}\left[\frac{w_0}{h} + 0{\cdot}512\left(\frac{w_0}{h}\right)^3\right]. \tag{13}$$

An alternative solution for the clamped plate, but with boundary conditions that allow movement of the edge in the radial direction, is given by Prescott (1924) in a more general form with the value of ν unassigned. This may be expressed

$$\frac{qa^4}{Eh^4} = \frac{16}{3(1-\nu^2)}\ \frac{w_0}{h} + \frac{6}{7}\left(\frac{w_0}{h}\right)^3. \tag{14}$$

It is assumed that these two theoretical extremes will bracket the real edge condition of the area of gut cell cortex outlined by the *Giardia* ventral disc rim where free movement of the 'edge' will depend on the tangential extensibility of the adjacent epithelial surface.

CALCULATION OF THE RESULT

Suction pressure attached to glass

The reservations appended to the results of Table 1 make it clear that the status of these data do not allow direct extrapolation to a physiological situation. In the gut a faster wave velocity than has been measured might be expected at higher temperature. Also, in the following calculations the viscosity of the medium is assumed as for water,

Table 2. *Calculation of* Giardia *suction pressure from flagellar wave parameters*

Frequency (Hz)	Assumed waveform	Propulsive velocity,* u_{max} (μm sec^{-1})	Suction pressure,† ΔP (dynes cm^{-2})
18	Helical	5·8	124
18	Plane-sine	3·8	84
2·5	Helical	1·4	31
2·5	Plane-sine	1·0	22

* From equation (10) or (11); $d = 0{\cdot}3$ μm, $m = 4$.

† From equation (2) with the following values assigned: $n = 0{\cdot}5$; $\mu = 10^{-2}$ poise, $\iota = \frac{3}{4}\pi R_D$, $R_D = 4{\cdot}12$ μm, $r = 0{\cdot}1$ μm.

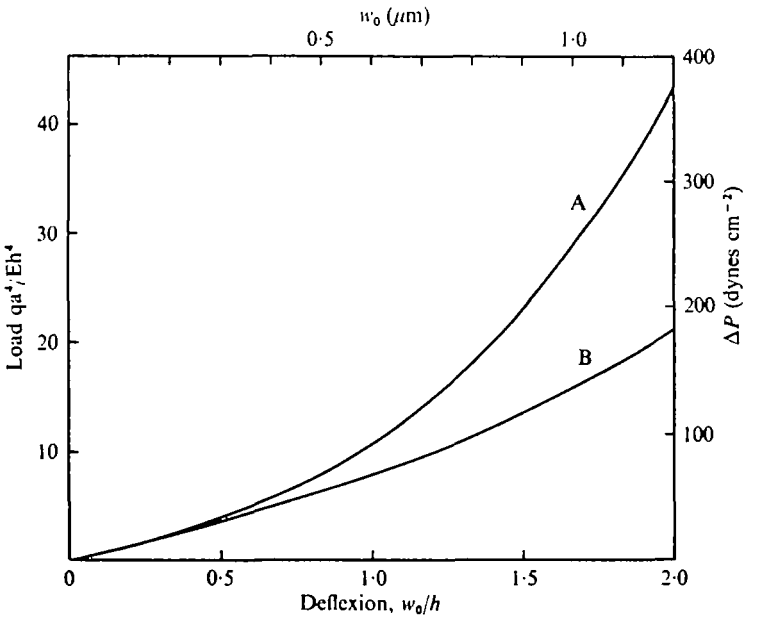

Text-fig. 5. Load-deflexion curves for: *A*, a rigidly clamped circular plate (equation 13), and *B*, a plate with radial edge movement (equation (14); $\nu = 0{\cdot}5$). Top and right-hand scales relate deflexion (w_0) of a gut-cell cortex of thickness (h) = 0·6 μm to suction pressure (ΔP) within a *Giardia* disc of radius 3·5 μm.

and this is likely to be less than the real fluid viscosity close to the gut wall. On both counts a value of suction pressure calculated from equation (2) using these values will underestimate the range of suction pressure that might be achieved *in situ*. None the less the flagellates attach to glass and subsequently detach when flagellar beating is sufficiently slowed, and this more narrowly defined event may be satisfactorily analysed. Table 2 summarizes the result of substituting into equation (2) representative values of the channel parameters averaged from at least 20 electron micrographs, and alternative values of u_{max} calculated from equations (10) and (11) for helical and plane waves using the first and last lines of Table 1. The result fixes an upper limit on the suction pressure permitted by present observations, and a lower limit compatible with maintained attachment to glass.

Suction pressure attached to the gut epithelium

Of the parameters appearing in the bent-plate formulae (13) and (14), a, w_0 and h may be measured directly from micrographs (Pl. 1, fig. 2). A problem of interpretation attaches to the measurement of the plate thickness, h, in deciding where lies the boundary between the effective elastic cortex and the internal fluid cytoplasm of the epithelial cell. For the present the cortex may be identified with a discrete layer beneath the brush border, in electron micrographs marked by fine microfilaments. The brush border itself, a highly corrugated sheet, offers minimal resistance to bending and is not considered part of the effective plate. Text-fig. 5 plots the dependence of the central deflexion on suction pressure for the two cases expressed in equations (13) and (14), from likely values of the relevant parameters. A complete solution for suction pressure rests with finding Young's modulus for the gut cell cortex. Making the assumption that this value for a 'cortical' cell such as the epithelial cell compares with Young's modulus for another 'cortical' cell, the unfertilized sea-urchin egg ($E = 10^4$ dynes cm^{-2}; Mitchison & Swann, 1954), a central deflexion of 0·7 μm would be produced by a suction pressure of 122 dynes cm^{-2} in the case of a rigidly clamped cortical disc, 83 dynes cm^{-2} allowing for radial edge movement. The largest central deflexion that has been measured from micrographs is 0·76 μm.

DISCUSSION

The foregoing analysis of the hydrodynamic model provides a good agreement between the range of suction pressures developed by *Giardia* attaching to glass and the least suction pressure that must be invoked to account for the local curvature of the gut epithelium in electron micrographs. The following limitations of the result argue caution in accepting this agreement at face value.

(1) In that the treatment of fluid flow around the flagella rests with the general arguments of Gay and Hancock and ignores the complexity of channel flow, the result for propulsive velocity must be approximate. Also, though both plane and helical waves have been considered, in each case the flagellar waveform has been assumed uniform. In reality the wavelength increases from base to tip by a factor of 2. The wave amplitude may also be non-uniform, particularly at low frequency when the ratio of extremes may be 1·6. In these cases the amplitude increases with wavelength as the wave passes distally along the paired flagellar shafts.

(2) The gut cell cortex has been treated as an isolated plate for which the load applied to its face is balanced only by stresses arising within its arbitrarily defined perimeter.

(3) A value of Young's modulus has been assumed for the gut cell cortex and may not be justifiable.

On the first point, the errors due to non-uniformity of flagellar motion are likely to be small in comparison to those introduced by the simplicity of the hydrodynamic argument. Holwill & Miles (1971) and Coakley & Holwill (1972) have calculated by protracted numerical integration the propulsive velocity of non-uniform plane and three-dimensional flagellar waves for a number of representative cases, and compared the results over a range of ηk values with the approximate solution provided b

e substitution of mean wave parameters into the formulae of Gray & Hancock (1955) and Holwill & Burge (1963). The error incurred through the use of the approximate formulae is significant only if the scale of the non-uniformity is greater than a factor of 2, becomes increasingly so as the value of ηk increases, but is reduced considerably by the presence of a large inert body. The greatest error from this source in the stated result of *Giardia* (Table 2) will be found in the calculations at slower frequencies ($\eta k > 1{\cdot}5$), which are in any case uncertainly related to the behaviour of flagellates *in situ*.

The bent plate equations may be tested against a known experimental result, the deformation of the sea-urchin egg in an elastimeter (Mitchison & Swann, 1954). If account is taken of increased plate area as more egg surface is recruited into the elastimeter tip under greater suction pressure, the equations give linear pressure-deformation curves that bracket the experimental points (Holberton (1973), unpublished calculations). The fit is not altogether surprising since Mitchison and Swann conclude that tangential tension in the complete cortex is much less significant than local bending stresses at the elastimeter tip. In the first instance this exercise justifies the bent plate analysis, and secondly confirms the value of Young's modulus derived by these authors from model experiments. Recently the validity of results from elastimeter experiments has been challenged by Mela (1967), who suggests 10^7 as a more likely value of Young's modulus, and one that accords with results from other tissue sources, such as spermatozoa tails, collagen and erythrocytes, that generally fall within the range 10^7 to 10^8. The basis of Mela's determination of the elastic modulus was the swelling behaviour of sea-urchin eggs under osmotic stress, and the discrepancy between the two values is probably inherent in the different experimental approaches. The elastimeter measures local cortical bending whereas the principal stress of a swollen egg is circumferential tension. If in the latter case once the membrane has been unfolded by initial swelling (the 'elastic domain' of Mela) resistance is offered to a large extent by the membrane itself and not the cortex, then the result might be expected to agree with a 'pure membrane' measurement such as elastimetry of the erythrocyte surface (Rand, 1964). A distinction may here need to be drawn between 'cortical' surfaces and 'membrane' surfaces. Cells such as the sea-urchin egg or the newt egg (Selman & Waddington, 1955) which give a modulus of order 10^4 to 10^5 by elastimetry are also identified by a thick submembrane cortex (Mitchison, 1956) within which actin-like filaments assemble locally during cleavage (Tilney & Marsland, 1969; Perry, John & Thomas, 1971). The discrete filament-containing periphery of the intestinal epithelial cell suggests that it might reasonably be allied with this group.

The hydrodynamic model raises a point of biological significance. Assuming a reasonably constant fluid velocity from sustained flagellar beating, suction pressure is critically dependent on the shape adopted by the lateral flange, both in the absolute length channelling the flow, and, more importantly, in the vertical separation of the flange arch from the substrate (Text-fig. 3). For example, should the flange be raised by 0·5 μm (from a resting separation of 0·2 μm) suction pressure would fall from 120 to less than 10 dynes cm^{-2}, an effect that compares with slowing the rate of beating from 20 to 1·75 Hz. Ultimately detachment from a surface might be accomplished by this means. The control of flange shape has previously been attributed to a 'paramyosin-like' marginal plate within its cytoplasm (Friend, 1966). The model

advanced here predicts that for part of its length the flange develops an arched profile and maintains this shape against pressure collapse over extended periods. Though detailed evidence is lacking to confirm the identity of the flange plate, these properties would be manifest in a contractile system embodying a 'catch' mechanism. The extent to which contractile proteins familiar from metazoan sources are anticipated at the protozoan level is indicated by some recent discussions of protozoan contractile systems (Pollard, Shelton, Weihing & Korn, 1970; Holberton & Preston, 1970; Nachmias, 1972). Though conservative evolution of actomyosin systems is implied by hybrid actomyosins formed from plasmodial actin and rabbit myosin (Nachmias, Huxley & Kessler, 1970), there is also evidence of a contractile system peculiar to protozoa in the elastic recoil mechanism of peritrich spasmonemes (Weiss-Fogh & Amos, 1972).

SUMMARY

1. The attachment of *Giardia* trophozoites can be modelled by viscous-flow equations demonstrating that a suction pressure arises from the viscous stress of a fluid flow led beneath the cell by flagellar activity.

2. Changing fluid velocity is less significant in generating suction.

3. Over the range of flagellar wave parameters observed from cells attached to glass, suction pressure may reach 10^2 dynes cm^{-2}.

4. Expressions for the bending of a thick disc under normal load allow an estimate of suction pressure *in situ* from its deforming effect on the gut-cell cortex. Allowing for alternative boundary states, calculations suggest that suction pressures close to 10^2 dynes cm^{-2} account for the deformations measured from electron micrographs.

5. The shape assumed by a ventro-lateral flange determines the magnitude of the developed suction pressure and may constitute a control mechanism of attachment and detachment.

I would like to thank Dr R. B. Ginder for the critical reading of the manuscript. This work was supported by a grant from the Science Research Council.

REFERENCES

COAKLEY, C. J. & HOLWILL, M. E. J. (1972). Propulsion of micro-organisms by three-dimensional flagellar waves. *J. theor. Biol.* **35**, 525–42.

CURTIS, A. S. G. (1967). *The Cell Surface: Its Molecular Role in Morphogenesis*. London: Logos Press.

DUNCAN, W. J., THOM, A. S. & YOUNG, A. D. (1970). *Mechanics of Fluids*, 2nd ed. London: Edward Arnold.

FRIEND, D. S. (1966). The fine structure of *Giardia muris*. *J. Cell Biol.* **29**, 317–32.

GRAY, J. & HANCOCK, G. J. (1955). The propulsion of sea-urchin spermatozoa. *J. exp. Biol.* **32**, 802–14.

HOLBERTON, D. V. (1973). Fine structure of the ventral disc apparatus and the mechanism of attachment in the flagellate *Giardia muris*. *J. Cell Sci.* (in the Press).

HOLBERTON, D. V. & PRESTON, T. M. (1970). Arrays of thick filaments in ATP-activated *Amoeba* model cells. *Expl. Cell Res.* **62**, 473–7.

HOLWILL, M. E. J. (1966). Physical aspects of flagellar movement. *Physiol. Revs.* **46**, 696–785.

HOLWILL, M. E. J. & BURGE, R. E. (1963). A hydrodynamic study of the motility of flagellated bacteria. *Archs Biochem. Biophys.* **101**, 259–60.

HOLWILL, M. E. J. & MILES, C. A. (1971). Hydrodynamic analysis of non-uniform flagellar undulations. *J. Theor. Biol.* **31**, 25–42.

MELA, M. J. (1967). Elastic-mathematical theory of cells and mitochondria in swelling process. I. The membranous stresses and modulus of elasticity of the egg cell of sea urchin, *Strongylocentrotus purpuratus*. *Biophys. J.* **7**, 95–110.

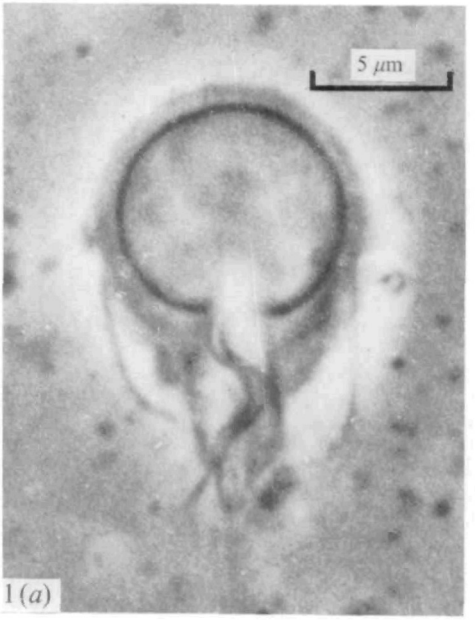
5 μm
1(a)

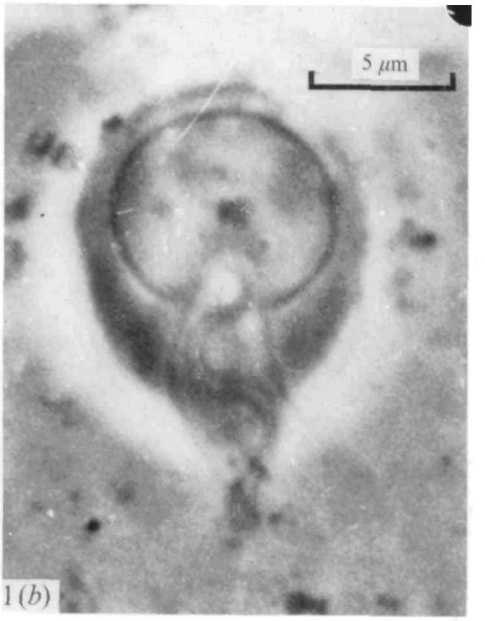
5 μm
1(b)


1 μm
w
h
2

MITCHISON, J. M. (1956). The thickness of the cortex of the sea urchin egg and the problem of the vitelline membrane. *Q. Jl Microsc. Sci.* **97**, 109–21.

MITCHISON, J. M. & SWANN, M. M. (1954). The mechanical properties of the cell surface. I. The cell elastimeter. *J. exp. Biol.* **31**, 443–60.

NACHMIAS, V. T. (1972). Filament formation by purified *Physarium* myosin. *Proc. natn. Acad. Sci. U.S.A.* **69**, 2011–14.

NACHMIAS, V. T., HUXLEY, H. E. & KESSLER, D. (1970). Electron microscope observations on actomyosin and actin preparations from *Physarum polycephalum*, and on their interaction with heavy meromyosin subfragment I from muscle myosin. *J. molec. Biol.* **50**, 83–90.

PAI, S. (1956). *Viscous Flow Theory*. Vol. I. *Laminar Flow*. Princeton: D. van Nostrand.

PERRY, M. M., JOHN, H. A. & THOMAS, N. S. T. (1971). Actin-like filaments in the cleavage furrow of newt egg. *Expl Cell Res.* **65**, 249–53.

POLLARD, T. D., SHELTON, E., WEIHING, R. R. & KORN, E. D. (1970). Ultrastructural characterization of F-actin isolated from *Acanthomoeba castellanii* and identification of cytoplasmic filaments of F-actin by reaction with rabbit heavy meromyosin. *J. molec. Biol.* **50**, 91–7.

PRESCOTT, J. (1924). *Applied Elasticity*. (Dover edition, 1961). New York: Dover Publications Inc.

RAND, R. P. (1964). Mechanical properties of the red cell membrane. II. Viscoelastic breakdown of the membrane. *Biophys. J.* **4**, 303–16.

SELMAN, G. G. & WADDINGTON, C. H. (1955). The mechanism of cell division in the cleavage of the newt's egg. *J. exp. Biol.* **32**, 700–33.

SILVESTER, N. R. & HOLWILL, M. E. J. (1972). An analysis of hypothetical flagellar waveforms. *J. theor. Biol.* **35**, 505–23.

TAYLOR, G. I. (1951). Analysis of the swimming of microsopic organisms. *Proc. R. Soc. Lond.* A, **209**, 447–61.

TILNEY, L. G. & MARSLAND, D. (1969). A fine structural analysis of cleavage induction and furrowing in the eggs of *Arbacia punctulata*. *J. Cell. Biol.* **42**, 170–84.

TIMOSHENKO, S. (1937). *Vibration Problems in Engineering*, 2nd ed. London: Constable.

TIMOSHENKO, S. & WOINOWSKY-KRIEGER, S. (1959). *Theory of Plates and Shells*, 2nd ed. New York: McGraw-Hill.

WEISS-FOGH, T. & AMOS, W. B. (1972). Evidence for a new mechanism of cell motility. *Nature, Lond.* **236**, 301–4.

YONEDA, M. (1964). Tension at the surface of sea-urchin egg: A critical examination of Cole's experiment. *J. exp. Biol.* **41**, 893–906.

EXPLANATION OF PLATE

Fig. 1. Phase-contrast micrographs of *Giardia* trophozoites attached to glass. The synchronous wave form of the two ventral flagella within the ventro-caudal channel is evident. Flagellar frequency: (*a*) 12 Hz, (*b*) 7 Hz.

Fig. 2. Electron micrograph of a trophozoite *in situ* on the mouse gut wall. The section is taken obliquely and anterior to the plane of Text-fig. 2; the deflexion of the epithelium (*w*) is not the true central deflexion. On one side the protozoan shares a ventro-lateral channel with a neighbouring organism (arrow). The cortical plasm defines a plate of thickness, *h*.